

See discussions, stats, and author profiles for this publication at: <https://www.researchgate.net/publication/51244099>

# Interactive Configuration through Force Analysis of GM1 Pentasaccharide–Vibrio cholera Toxin Interaction

ARTICLE *in* ANALYTICAL CHEMISTRY · JUNE 2011

Impact Factor: 5.64 · DOI: 10.1021/ac201013p · Source: PubMed

---

CITATIONS

7

---

READS

27

5 AUTHORS, INCLUDING:



**Chang Sup Kim**

Yeungnam University

27 PUBLICATIONS 157 CITATIONS

SEE PROFILE



**Hyung Joon Cha**

Pohang University of Science and Technology

196 PUBLICATIONS 2,537 CITATIONS

SEE PROFILE

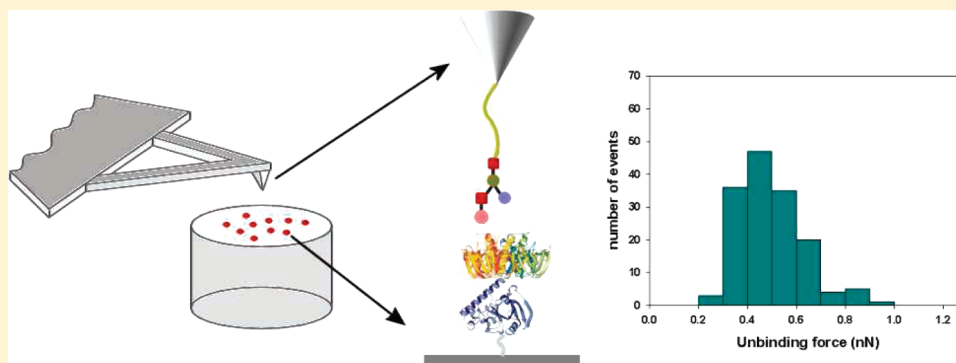
# Interactive Configuration through Force Analysis of GM1 Pentasaccharide-*Vibrio cholera* Toxin Interaction

Jeong Hyun Seo,<sup>†,‡</sup> Chang Sup Kim,<sup>†</sup> Hea Yeon Lee,<sup>§</sup> Tomoji Kawai,<sup>§</sup> and Hyung Joon Cha<sup>\*,†</sup>

<sup>†</sup>Department of Chemical Engineering, Pohang University of Science and Technology, Pohang 790-784, Korea

<sup>§</sup>Institute of Scientific and Industrial Research, Osaka University, Osaka 567-0047, Japan

## ABSTRACT:



Understanding of the molecular relationships in carbohydrate–protein interactions provides useful information on biological processes in living organisms and is also helpful for development of potent biomedical agents. Herein, the interaction unbinding force between GM1 pentasaccharide and *Vibrio cholera* toxin (ctx) proteins was measured using atomic force microscopy (AFM), which enabled us to determine the interaction of ctx holotoxin (ctxAB) with GM1 and the interactive formation. First, the interaction force measured between A and B subunits (ctxA–ctxB) was  $184.2 \pm 4.5$  pN, and the unbinding forces were evaluated to confirm the role of ctxA in ctxAB complex formation and were determined to be  $443.7 \pm 7.5$  and  $535.7 \pm 25.9$  pN for GM1–ctxB and GM1–ctxAB complexes, respectively. The force difference of  $\sim 90$  pN between GM1–ctxB and GM1–ctxAB might be due to the formation of the cholera toxin complex. Importantly, from the analogue analyses, we understand how structural and binding positional differences in complex carbohydrates affect the interaction with protein and surmise that the GM1–ctxAB complex makes a “two-finger grip” formation through the conformational change of a flexible carbohydrate. In conclusion, using AFM force analysis, we successfully quantified and characterized the interactive configuration of carbohydrate–protein molecules.

## INTRODUCTION

Traditionally, the interactions between particles or molecules have been analyzed in bulk; that is, interactions between many molecules were examined at the same time. Thus, the result was always the ensemble average of the behavior of individual molecules. The actual behavior of the individual molecule could not be known and had to be deduced from their collective behaviors. Thus, quantitative analytical methods for determining the behavior of individual molecules, such as scanning probe microscopy, optical tweezers, biomembrane force probes, and flexible microneedles, have been devised.<sup>1–4</sup> In particular, with these instruments, a force can be applied to an individual molecule to examine the bonds holding the structure together. Clearly, these measurements have added novel and complementary information to traditional bulk experiments.

Atomic force microscopy (AFM) is not only a tool to image the topography of solid surfaces at high resolution, but it also can be used to measure force-versus-distance curves.<sup>5–18</sup> Force curves can provide valuable information on local material properties such as elasticity, hardness, adhesion, and surface charge densities. In the

initial stages, this force measurement technique has allowed accurate measurements of surface and intermolecular forces and has led to improved understanding in this field. Forces are recorded using AFM by monitoring the deflection of a cantilever as a probe that is brought into and out of contact with the sample. The data retrieved from the deflection of the cantilever is then used to create an illustration of force termed a force–distance curve.<sup>9,18–20</sup> It should be noted that such force measurements are performed in liquid environments to eliminate capillary forces that would otherwise mask the biomolecular interactions of interest.<sup>21</sup>



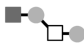

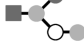
Among biomolecular interactions, carbohydrate–protein interactions play critical roles in living organisms, such as in cell–cell communication, signaling, cell adhesion, fertilization, and immunological processes.<sup>22–25</sup> These interactions also initiate infection of host cells by bacterial toxin proteins and viruses.<sup>26–29</sup> Thus, comprehensive studies on carbohydrate–protein interactions

Received: April 20, 2011

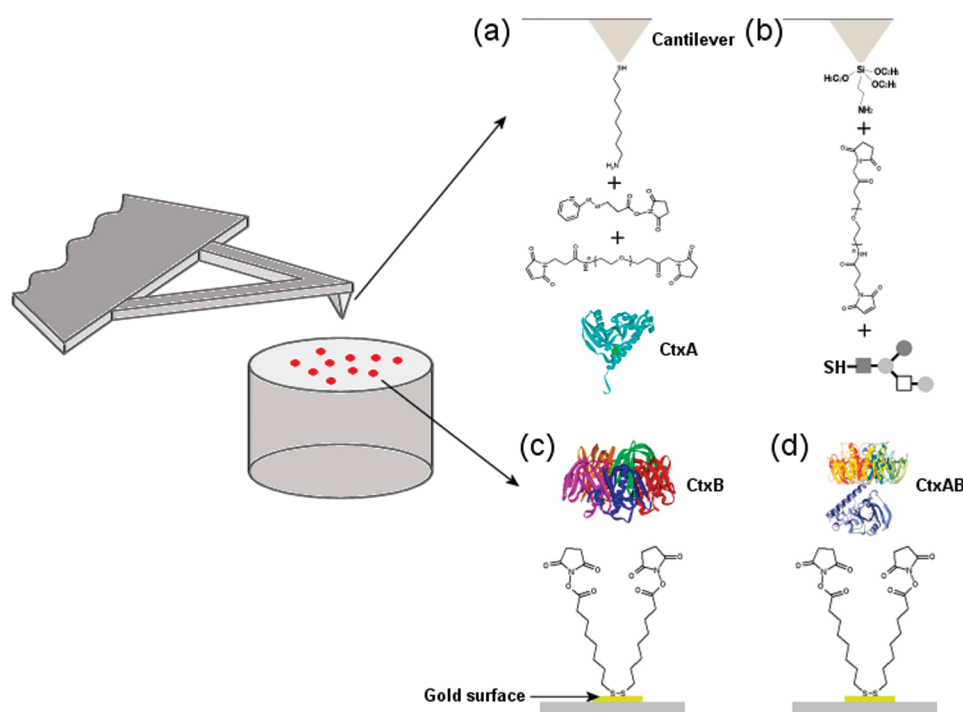
Accepted: June 24, 2011

Published: June 24, 2011

Table 1. Carbohydrates and Their Sequences Used in the Present Work

Glycan	Saccharide	Sequence	Symbol <sup>a</sup>
Lactose	disaccharide	Gal $\beta$ 1-4Glc	
GM1	pentasaccharide	Gal $\beta$ 1-3GalNAc $\beta$ 1-4(Neu5Ac $\alpha$ 2-3)Gal $\beta$ 1-4Glc	
Asialo GM1	tetrasaccharide	Gal $\beta$ 1-3GalNAc $\beta$ 1-4Gal $\beta$ 1-4Glc	
GM3	trisaccharide	Neu5Ac $\alpha$ 2-3Gal $\beta$ 1-4Glc	
Lstb	pentasaccharide	Gal $\beta$ 1-3GlcNAc $\beta$ 1-3(Neu5Ac $\alpha$ 2-6)Gal $\beta$ 1-4Glc	

<sup>a</sup> Symbol legend: dark gray squares represent glucose; light gray circles represent galactose; dark gray circles represent *N*-acetylneuraminic acid; open squares ( $\square$ ) represent *N*-acetylgalactosamine; and open circles ( $\circ$ ) represent *N*-acetylglucosamine.



**Figure 1.** Schematics of cantilever tip modification and surface preparation for immobilization of biomolecules. Immobilizations of (a) ctxA on Au-coated cantilever tip, (b) thiol-modified carbohydrates on silica nitride cantilever tip, and (c) ctxB and (d) ctxAB on gold surfaces.

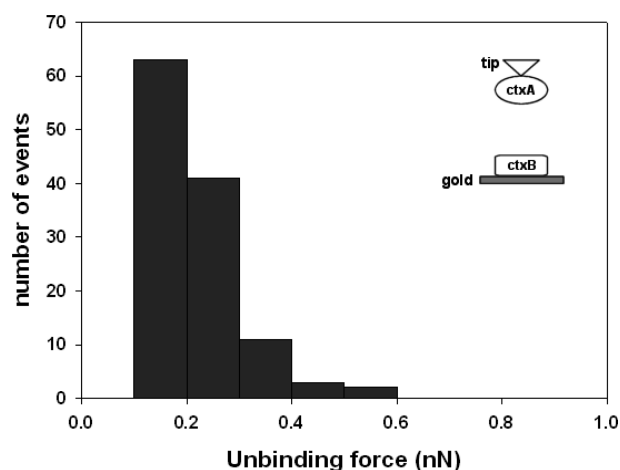
could provide useful information on screening and development of potent biomedical agents and on biological processes in living organisms.<sup>26,30,31</sup>

The interaction between ganglioside GM1 and *Vibrio cholera* toxin (ctx) proteins has been generally regarded as a good model for carbohydrate–protein interactions.<sup>32</sup> Until now, although several results describing the interaction of ganglioside GM1-*V. cholera* toxin B subunit (ctxB) have been reported,<sup>33–39</sup> there are few reports on its exact interaction force. Measurement of the interaction force between ctxB and GM1 was reported,<sup>40</sup> but the use of a relatively weak hydrophobic interaction for saccharide immobilization might be unreliable for identifying the unbinding position. In addition, a study on the participating A subunit (ctxA) was reported using flow cytometry with the simple description that the binding of the entire toxin (ctxAB)

is stronger than the binding of ctxB alone.<sup>36</sup> Consequently, revealing the clear interaction mechanism for ganglioside GM1, ctxA, ctxB, and ctxAB through direct measurement of the interaction force would be a very meaningful work. In the present work, to provide valuable information about intrinsic relationships, we employed AFM as a tool for direct measurements of the interaction force between GM1 pentasaccharide and *V. cholera* toxin proteins.

## EXPERIMENTAL SECTION

**Materials.** Lactose and aminophenyl disulfide were purchased from Sigma–Aldrich (St. Louis, MO, USA), and dimethylamino borane was obtained from Fluka (St. Louis, MO, USA). GM1 analogues (Table 1) used for carbohydrate modification consisted

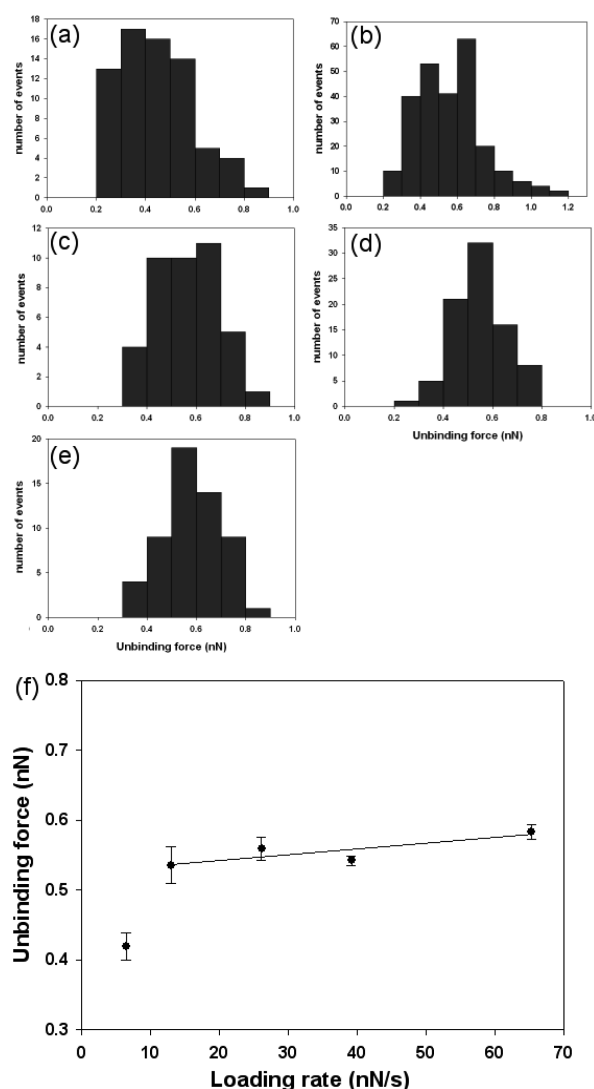


**Figure 2.** Force histogram ( $n = 120$ ) for the interaction of cholera toxin  $\text{ctxA}$  and  $\text{ctxB}$ . Force measurements were performed with a loading rate of  $13.08 \text{ nN/s}$ .

of the following: GM1 pentasaccharide from Enzo Life Sciences (Plymouth Meeting, PA, USA),  $\beta$ 1–3 galactosyl-*N*-acetyl galactosaminyl- $\beta$ 1–4 galactose- $\beta$ 1–4 glucose (asialo GM1) from V-Laboratories (Covington, LA, USA), and 3-sialyllactose (GM3) and LS-tetrasaccharide b (Lstb) from Glyko (Novato, CA, USA). A silicon nitride ( $\text{Si}_3\text{N}_4$ ) cantilever was purchased from Veeco Probes (Santa Barbara, CA, USA). Coupling reagents for carbohydrate and protein immobilization consisted of the following: (3-aminopropyl)-triethoxy silane from Sigma, 8-amino-1-octanethiol *N*-succinimidyl 3-(2-pyridyldithio)propionate and dithiobis (succinimidyl octanoate) from Dojindo (Kumamoto, Japan), and MAL-dPEG<sub>24</sub>-NHS ester from Quanta Biodesign (Powell, OH, USA). HBS-EP buffer and dithiothreitol (DTT) were purchased from GE Healthcare (New York, NY, USA) and USB Corp. (Cleveland, OH, USA), respectively. Cholera toxin  $\text{ctxA}$  and  $\text{ctxB}$  proteins were purchased from Sigma–Aldrich.

**Carbohydrate Modification.** Carbohydrate modification followed the same protocol developed in the previous work.<sup>40</sup> Lactose (100 or 50 mM) and GM1 analogues (GM1, asialo GM1, GM3, and Lstb) were separately dissolved in deionized water, and 50 mM aminophenyl disulfide was dissolved in glacial acetic acid. Then, carbohydrate and aminophenyl disulfide solutions were mixed sufficiently and incubated in sealed tubes for 1 h at  $30^\circ\text{C}$  for reductive amination coupling. To quench the reaction, freshly prepared reducing reagent, 100 mM dimethylamine borane, was added to each reaction, and the tubes were incubated unsealed for 1 h at room temperature. Each product was evaporated under nitrogen gas streaming by heating for 1 h at  $50^\circ\text{C}$  for condensation. Finally, all modified carbohydrates were dissolved in the proper solution (distilled water or HBS-EP buffer) and preserved at  $-20^\circ\text{C}$  in dark conditions. Without further purification steps, modified carbohydrates were used for matrix-assisted laser desorption/ionization mass spectrometry (MALDI-TOF MS) analysis and immobilized onto an AFM cantilever.

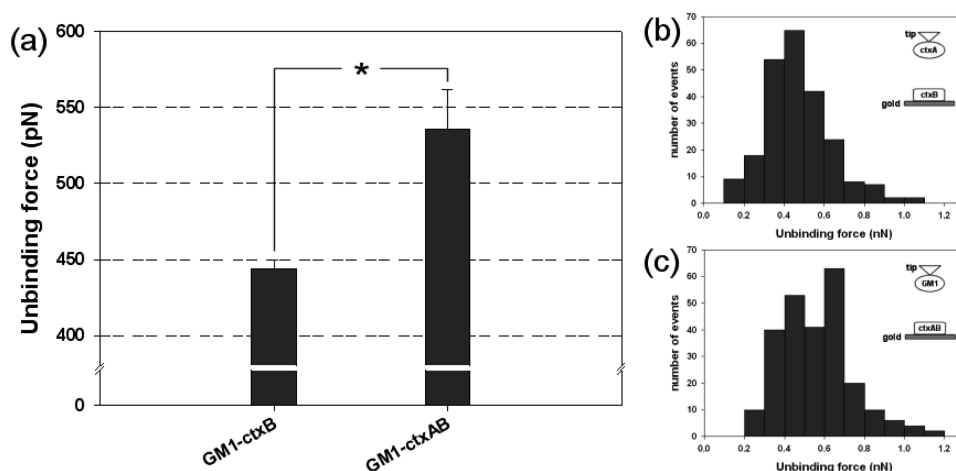
**Cantilever Tip Modification for Biomolecule Immobilization.** Gold-coated silicon nitride cantilever tips were cleaned in an  $\text{O}_2$  plasma for 1 h and then transferred into 5 mM 8-amino-1-octanethiol in a saturated envelope for 12 h, resulting in aminothiolfunctionalized tips. In a similar way, bare silicon nitride cantilever tips were cleaned and then transferred into (3-aminopropyl)-triethoxy silane, resulting in aminosilane-functionalized tips.



**Figure 3.** Dependence of the unbinding forces on the loading rates for the interaction of GM1 pentasaccharide with  $\text{ctxAB}$ : (a–e) force histograms according to the loading rates of  $6.54 \text{ nN/s}$  (panel a),  $13.08 \text{ nN/s}$  (panel b),  $26.16 \text{ nN/s}$  (panel c),  $39.24 \text{ nN/s}$  (panel d), and  $65.4 \text{ nN/s}$  (panel e). (f) Correlation between unbinding forces and loading rates (the line in panel e represents a simple linear fit).

The aminated gold-coated tips were additionally functionalized with 1 mM *N*-succinimidyl 3-(2-pyridyldithio)propionate in HBS-EP buffer for 1 h and treated with 50 mM DTT to terminate the thiol group for 20 min. Then, both aminated gold-coated and bare tips were functionalized with 1 mM of MAL-dPEG<sub>24</sub>-NHS ester in HBS-EP buffer for 1 h. After washing two times with HBS-EP buffer,  $\text{ctxA}$  subunits and thiolated saccharides were finally treated on functionalized gold-coated and bare silicon nitride cantilever tips, respectively, for 2 h. To prevent evaporation of the linker and biomolecule solutions, immobilized cantilevers were incubated in a humidity chamber. Immobilizations of the  $\text{ctxA}$  protein and the thiolated-saccharide on functionalized cantilever tips are illustrated in Figures 1A and 1B, respectively.

**Surface Preparation.** The gold (Au) surface was prepared by sputtering high-purity gold onto a  $\text{SiO}_2$  wafer presonicated in ethanol with a titanium (Ti) adhesion layer (100 nm Au



**Figure 4.** (a) Interaction forces measured between GM1–ctxB ( $n = 231$ ) and GM1–ctxAB ( $n = 498$ ) and force histograms for (b) GM1–ctxB and (c) GM1–ctxAB. Force measurements were performed with a constant loading rate of 13.08 nN/s. Values and error bars represent the means of samples and standard deviations with statistical significance. (In panel a, the asterisk (\*) indicates  $p < 0.001$ .)

and 5 nm Ti). The gold surface was immersed into 1 mM dithiobis (succinimidyl octanoate) in acetonitrile for 1 h and subsequently cross-linked with cholera toxin ( $20 \mu\text{g mL}^{-1}$ ) after cleaning with HBS-EP buffer (illustrated in Figure 1C for ctxB and Figure 1D for ctxAB). To allow possible formation of complexes such as ctxB<sub>5</sub> and ctxAB<sub>5</sub>, cholera toxin subunits were premixed for at least 48 h at 4 °C.

**AFM Force Measurement.** Measurements were carried out on a Nanoscope IIIa/Multimode AFM (Digital Instruments, Santa Barbara, CA, USA) that was operated in aqueous phase at ambient temperature in force volume mode. Force spectroscopy experiments were performed in HBS-EP buffer with retraction speeds from  $50 \text{ nm s}^{-1}$  to  $500 \text{ nm s}^{-1}$ . Obtained data were processed using SPIP V3.3.7.0 software (Image Metrology, Lyngby, Denmark), and unbinding forces were calculated manually by Hooke's law ( $F = -kx$  (where  $F$  is the force,  $k$  the spring constant, and  $x$  the distance)). Each force was rearranged to form a histogram of force versus the number of events, and finally, the unbinding force was evaluated.

## RESULTS AND DISCUSSION

**Interaction Force Analysis between Toxin A and B Subunits.** Even though ctxA is known to be a requirement to achieve appreciable cell binding and to trigger downstream events,<sup>37,41,42</sup> the direct interaction force between the two toxin proteins, ctxA and ctxB, has not been determined yet. First, we performed AFM analysis to obtain force curves for the ctxA–ctxB interaction. The N-terminus of ctxB, which is not an active site for the ctxA–ctxB interaction,<sup>43–45</sup> was covalently immobilized on the gold surface with an NHS ester of dithiobis (succinimidyl octanoate) (Figure 1c). Also, three different linkers were attached to the AFM cantilever to create a flexible space, and then ctxA was covalently attached on the linker terminus (Figure 1a). After obtaining repeated force curves, unbinding forces were calculated and sorted by histogram analysis to determine the rupture force ( $n = 120$ ; see Figure 2). We applied a bin size of 50 pN to determine the rupture force of the interaction (note that the histogram in Figure 2 is shown with a bin size of 100 pN for consistency) and Gaussian peak analysis for the histogram to calculate interaction force. The equation for the Gaussian

peak analysis is

$$F = a \exp \left[ -0.5 \left( \frac{(X - X_0)}{b} \right)^2 \right] \quad (1)$$

where  $a$  and  $b$  are the coefficients to be determined to obtain the prescribed autocorrelation function.  $X_0$  is the average of  $X$  (rupture force) values within measured forces. Since there is no “best” number of bins, and different bin sizes can reveal different features of the data,<sup>46</sup> we determined the bin size by the standard method of Scott's rule ( $h = 3.5sN^{-1/3}$ , where  $h$  is the bin size,  $s$  the standard deviation, and  $N$  the number of data).<sup>47</sup> From this equation, we obtained a bin size of approximately 50 pN and used this bin size in the sorting software. Using a bin number of 50 pN, we determined the interaction force between ctxA and ctxB to be  $184.2 \pm 4.5 \text{ pN}$  ( $P < 0.0001$ ). This interaction force is relatively similar to other ligand–receptor interactions.<sup>10,48–50</sup> This result might indicate that ctxA–ctxB binding is not comparably strong, although the formation of ctxAB complex is essential for the infection process.<sup>48,49,51</sup>

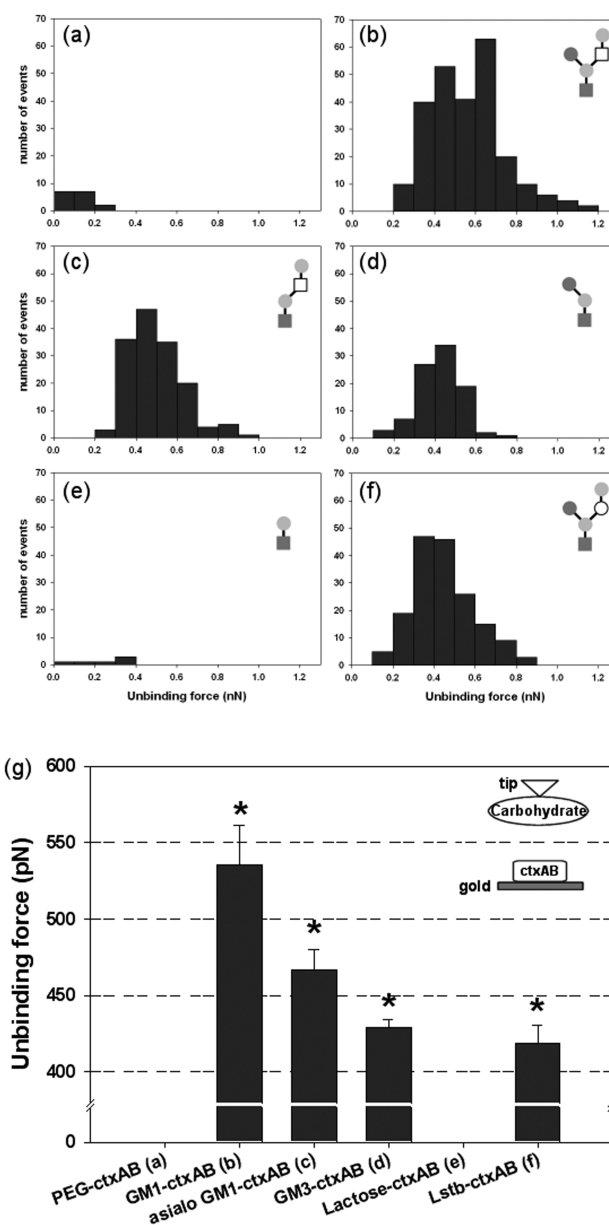
**Interaction Force Analysis for GM1 Pentasaccharide and Cholera Toxins.** In the present work, measurement of the unbinding force between a single carbohydrate and a protein was attempted. The direct interaction force between GM1 pentasaccharide (or ganglioside GM1) and cholera toxin ctxAB complex was not determined by AFM except for one trial in which a GM1–ctxB interaction was created using the hydrophobic method for immobilization of the carbohydrate on the tip.<sup>52</sup> Generally, for interaction force measurements of biomolecules, surface immobilization through covalent attachment is required.<sup>18</sup> In addition, relatively weak hydrophobic immobilization might make identification of the unbinding position difficult. Therefore, we utilized the covalent method for both carbohydrate and protein immobilization for measuring a reliable interaction force. After functionalizing the tip surface through  $\text{O}_2$  plasma cleaning, (3-aminopropyl)-triethoxysilane was covalently attached to the tip surface. A flexible linker, MAL-dPEG<sub>24</sub> NHS ester, was cross-linked with the amine group, and then finally, modified saccharides were attached onto the end of the NHS ester (Figure 1b). These modifications would provide strong linkage between linkers and saccharide.



First, we determined dependence of the unbinding force on the applied loading rate. By changing tip retraction speeds from  $50 \text{ nm s}^{-1}$  to  $500 \text{ nm s}^{-1}$ , loading rates from  $6.54 \text{ nN s}^{-1}$  to  $65 \text{ nN s}^{-1}$  were applied. The unbinding force had a linear correlation with the applied loading rate in the range of  $13\text{--}65 \text{ nN s}^{-1}$  (see Figure 3). This linear correlation indicates that the same potential barriers dominate the dissociation for all applied loading rates. Thus, from the subsequent experiments for interaction force measurements, we used the loading rate of  $13.08 \text{ nN s}^{-1}$ .

Next, we measured the interaction force between GM1 pentasaccharide and the cholera toxin ctxAB complex and evaluated the role of the A subunit within the GM1–ctxAB interaction by comparing with the interaction force of GM1 pentasaccharide–ctxB. Through the Gaussian peak analysis, the unbinding forces were evaluated as  $443.7 \pm 7.5$  for GM1–ctxB and  $535.7 \pm 25.9 \text{ pN}$  for GM1–ctxAB (see Figure 4a), which indicated relatively much higher interaction forces, compared to general ligand–receptor interaction forces.<sup>53</sup> In addition, because monosaccharides and their lectins have been generally used as model systems for measurements of carbohydrate–protein force interactions, due to the complexity and diversity of carbohydrates,<sup>54,55</sup> the results of the interaction force measurement for a complex structured carbohydrate and its receptor were very meaningful. In the case of GM1–ctxB, the histogram fit a Gaussian curve well (Figure 4b), but it was unreasonable to use a single Gaussian curve for the GM1–ctxAB analysis, because the histogram was divided into two parts near 450 and 550 pN (Figure 4c). Therefore, the force values could be analyzed as two unbinding forces. These patterns could be explained by the nonhomogeneous immobilization of ctxAB on the gold surface. Toxins ctxA and ctxB might not form the ctxAB complex effectively; thus, we suspect that the unbinding force of ctxB immobilized on the gold surface was also measured at the same time. We estimated the unbinding force between GM1 pentasaccharide and ctxAB to be  $535.7 \text{ pN}$ , and the second unbinding force at  $\sim 450 \text{ pN}$  is similar to that of GM1–ctxB ( $443.7 \text{ pN}$ ). Importantly, based on the force values obtained, we hypothesize that the force difference of  $\sim 90 \text{ pN}$  between GM1–ctxB and GM1–ctxAB is due to formation of cholera toxin protein complex.

**Interaction Force Analysis between GM1 Analogues and Cholera Toxin ctxAB Complex.** Comparative analyses using surface plasmon resonance and isothermal titration calorimetry have shown that *N*-acetylneuraminic acid (Neu5Ac) and the terminal galactose (Gal) residues of ganglioside GM1 pentasaccharide are the main contributors to the intrinsic binding energy of interaction with cholera toxin.<sup>32,35,37</sup> The unbinding force of the asialo GM1 analogue (see Table 1), which lacks the Neu5Ac from the GM1 structure, was measured as  $467.1 \pm 12.7 \text{ pN}$  (see Figures 5c and 5g). However, in the case of the GM3 analogue (Table 1), which lacks the Gal and *N*-acetyl galactosamine (GalNAc) from the GM1 structure, the unbinding force was slightly lower ( $429.3 \pm 4.9 \text{ pN}$ ) than the asialo GM1 analogue (see Figures 5d and 5g). These results demonstrate that the terminal saccharide moieties of ganglioside GM1 affect the force of binding to the toxin protein. As expected, when a noncarbohydrate (PEG linker only) and lactose (lack of Neu5Ac, Gal, and GalNAc from GM1 structure) were used as controls, no unbinding forces were measured (see Figures 5a, 5e, and 5g). Interestingly, Lstb (Table 1), which is a pentasaccharide with a structure similar to that of GM1 pentasaccharide, produced a fairly high unbinding force of  $418.5 \pm 12.4 \text{ pN}$ , which is much lower than that of GM1–ctxAB (Figures 5f and 5g). Therefore, a change of one



**Figure 5.** Force histograms for (a) PEG–ctxAB, (b) GM1–ctxAB, (c) asialo GM1–ctxAB, (d) GM3–ctxAB, (e) lactose–ctxAB, and (f) Lstb–ctxAB. (g) Force histogram of the interaction forces shown in panels a–f. Force measurements were performed with a loading rate of  $13.08 \text{ nN/s}$ . Values and error bars represent the means of samples and standard deviations with statistical significance (asterisk (\*) indicates  $p < 0.001$ ).

saccharide (*N*-acetyl glucosamine (GlcNAc) instead of GalNAc) and a different bond position of Neu5Ac (2–3 bond in GM1 vs 2–6 bond in Lstb) from the original GM1 structure are able to cause a decrease in the unbinding force of the carbohydrate–protein interaction, although both structures are apparently similar. The binding site between ctxB and GM1 pentasaccharide has been characterized using X-ray crystallography, and the crystal structure of the ctxB–GM1 complex contained a bivalent interaction of the branched GM1 pentasaccharide, which can be described as the carbohydrate holding the protein in a “two-fingered grip” comprising of a Neu5Ac thumb and a Gal–GalNAc forefinger.<sup>44</sup> Therefore, we surmise that the Lstb–ctxAB

interaction also produced a relatively high unbinding force, because of a structural similarity to the two-fingered grip.

Overall, simply based on the analogue comparisons, it may be not easy to conclude that the force differences between GM1–ctxAB and GM1 analogues–ctxAB interactions are from different sugar moieties. It was reported that, in terms of buried surface area, terminal Gal, GalNAc, and Neu5Ac residues contributed 39%, 17%, and 43% of intermolecular contacts, respectively.<sup>44</sup> Thus, the ~70 pN difference from the Neu5Ac deletion and the ~105 pN difference from the Gal and GalNAc deletion could not be explained by previously reported monosaccharide contributions. One explanation is that the flexible carbohydrate structure might interact with its lectin (here, ctxAB) by a complex formation similar to the two-finger grip through a conformational change, even though we found that their interactions are nonspecific by carbohydrate chip analysis.<sup>56</sup> The binding force result of the Lstb–ctxAB interaction might also support this hypothesis. Therefore, we surmise that the GM1–ctxAB complex needs a conformational change and appropriate space during its interaction.

## CONCLUSIONS

Herein, we analyzed interaction forces between carbohydrates and cholera toxins using atomic force microscopy (AFM). We, for the first time, measured the unbinding force (~184 pN) of ctxA and ctxB and found that ctxA–ctxB binding is not comparably strong, although the formation of the toxin protein ctxAB complex is essential for the infection process. The interaction force between the toxin protein and GM1 pentasaccharide (~536 pN) was increased by ~90 pN, because of the formation of the ctxAB complex compared to that between GM1 and the toxin protein ctxB (~444 pN). The results indicate that the unbinding force for the GM1–ctxAB complex was not critically increased, even though the binding of the entire toxin is stronger than the binding of ctxB alone. To investigate the roles of sugar moieties in the interaction, we measured unbinding forces for GM1 analogues. We found that the deletion of one or two sugars from GM1 analogues produced comparatively high unbinding forces with the toxin protein complex, while lactose, the three-sugars-deleted form of GM1 pentasaccharide, did not have an interaction force. Interestingly, the structurally similar Lstb pentasaccharide, which has GlcNAc instead of GalNAc, also produced a relatively high unbinding force, which might be from two anchored terminal monosaccharides (Neu5Ac–Gal) and a pentameric structural similarity. Therefore, we can surmise that Lstb does not bind to the cholera toxin in the same manner as the corresponding fragment of GM1 pentasaccharide, but rather it finds a higher affinity site elsewhere on the toxin protein. This might mean that the two-fingered grip formation is important in the interaction through a conformational change. However, structural differences and a change in one residue may severely affect the specificity of the carbohydrate to the cholera toxin. In conclusion, analysis of direct unbinding forces by AFM measurements produced reliable information about molecular structures. Therefore, AFM force analysis of biomolecular interactions is useful for identifying the structural roles in multivalent systems.

## AUTHOR INFORMATION

### Corresponding Author

\*Phone: +82 54 279 2280. Fax: +82 54 279 5528. E-mail: hjcha@postech.ac.kr.

### Present Addresses

<sup>†</sup>Department of Biomedical Engineering, University of California, Davis 95616, CA, USA.

## ACKNOWLEDGMENT

This work was supported by Technology Development Program for Agriculture and Forestry (No. 109187-3) from the Ministry for Agriculture, Forestry and Fisheries and the Engineering Research Center (2009-0079294) and the Brain Korea 21 Programs from the Ministry of Education, Science and Technology.

## REFERENCES

- (1) Kishino, A.; Yanagida, T. *Nature* **1988**, 334, 74–76.
- (2) Ashkin, A.; Schutze, K.; Dziedzic, J. M.; Euteneuer, U.; Schliwa, M. *Nature* **1990**, 348, 346–348.
- (3) Evans, E.; Ritchie, K.; Merkel, R. *Biophys. J.* **1995**, 68, 2580–2587.
- (4) Burnham, N. A.; Colton, R. J. *J. Vac. Sci. Technol.* **1989**, A7, 2906–2913.
- (5) Engel, A.; Muller, D. J. *Nat. Struct. Biol.* **2000**, 7, 715–718.
- (6) Benoit, M.; Gabriel, D.; Gerisch, G.; Gaub, H. E. *Nat. Cell Biol.* **2000**, 2, 313–317.
- (7) Clausen-Schaumann, H.; Seitz, M.; Krautbauer, R.; Gaub, H. E. *Curr. Opin. Chem. Biol.* **2000**, 4, 524–530.
- (8) Fisher, T. E.; Marszalek, P. E.; Fernandez, J. M. *Nat. Struct. Biol.* **2000**, 7, 719–724.
- (9) Florin, E. L.; Moy, V. T.; Gaub, H. E. *Science* **1994**, 264, 415–417.
- (10) Hinterdorfer, P.; Baumgartner, W.; Gruber, H. J.; Schilcher, K.; Schindler, H. *Proc. Natl. Acad. Sci. U.S.A.* **1996**, 93, 3477–3481.
- (11) Lee, G. U.; Chrisey, L. A.; Colton, R. J. *Science* **1994**, 266, 771–773.
- (12) Oberhauser, A. F.; Marszalek, P. E.; Erickson, H. P.; Fernandez, J. M. *Nature* **1998**, 393, 181–185.
- (13) Rief, M.; Clausen-Schaumann, H.; Gaub, H. E. *Nat. Struct. Biol.* **1999**, 6, 346–349.
- (14) Rief, M.; Gautel, M.; Oesterhelt, F.; Fernandez, J. M.; Gaub, H. E. *Science* **1997**, 276, 1109–1112.
- (15) Binnig, G.; Quate, C. F.; Gerber, C. *Phys. Rev. Lett.* **1986**, 56, 930–933.
- (16) Hoh, J. H.; Cleveland, J. P.; Prater, C. B.; Revel, J. P.; Hansma, P. K. *J. Am. Chem. Soc.* **1992**, 114, 4917–4918.
- (17) Willemsen, O. H.; Snel, M. M. E.; Cambi, A.; Greve, J.; De Grooth, B. G.; Figdor, C. G. *Biophys. J.* **2000**, 79, 3267–3281.
- (18) Hinterdorfer, P.; Dufrene, Y. F. *Nat. Methods* **2006**, 3, 347–355.
- (19) Moy, V. T.; Florin, E. L.; Gaub, H. E. *Science* **1994**, 266, 257–259.
- (20) Vinckier, A.; Gervasoni, P.; Zaugg, F.; Ziegler, U.; Lindner, P.; Groscurth, P.; Pluckthun, A.; Semenza, G. *Biophys. J.* **1998**, 74, 3256–3263.
- (21) Weisenhorn, A. L.; Hansma, P. K.; Albrecht, T. R.; Quate, C. F. *Appl. Phys. Lett.* **1989**, 54, 2651–2653.
- (22) Bertozi, C. R.; Kiessling, L. L. *Science* **2001**, 291, 2357–2364.
- (23) Ritchie, G. E.; Moffatt, B. E.; Sim, R. B.; Morgan, B. P.; Dwek, R. A.; Rudd, P. M. *Chem. Rev.* **2002**, 102, 305–319.
- (24) Roth, J. *Chem. Rev.* **2002**, 102, 285–303.
- (25) Zachara, N. E.; Hart, G. W. *Chem. Rev.* **2002**, 102, 431–438.
- (26) Sears, P.; Wong, C. H. *Angew. Chem. Int. Ed.* **1999**, 38, 2301–2324.
- (27) Boren, T.; Falk, P.; Roth, K. A.; Larson, G.; Normark, S. *Science* **1993**, 262, 1892–1895.
- (28) Lingwood, C. A. *Curr. Opin. Chem. Biol.* **1998**, 2, 695–700.
- (29) Simon, P. M.; Goode, P. L.; Mobasser, A.; Zopf, D. *Infect. Immun.* **1997**, 65, 750–757.
- (30) Danishefsky, S. J.; Allen, J. R. *Angew. Chem., Int. Ed.* **2000**, 39, 836–863.

- (31) Walter, F.; Vicens, Q.; Westhof, E. *Curr. Opin. Chem. Biol.* **1999**, *3*, 694–704.
- (32) Turnbull, W. B.; Precious, B. L.; Homans, S. W. *J. Am. Chem. Soc.* **2004**, *126*, 1047–1054.
- (33) Angstrom, J.; Teneberg, S.; Karlsson, K. P. *Natl. Acad. Sci. U.S.A.* **1994**, *91*, 11859–11863.
- (34) Fukuta, S.; Magnani, J. L.; Twiddy, E. M.; Holmes, R. K.; Ginsburg, V. *Infect. Immun.* **1988**, *56*, 1748–1753.
- (35) Kuziemko, G. M.; Stroh, M.; Stevens, R. C. *Biochemistry* **1996**, *35*, 6375–6384.
- (36) Lauer, S.; Goldstein, B.; Nolan, R. L.; Nolan, J. P. *Biochemistry* **2002**, *41*, 1742–1751.
- (37) MacKenzie, C. R.; Hiram, T.; Lee, K. K.; Altman, E.; Young, N. M. *J. Biol. Chem.* **1997**, *272*, 5533–5538.
- (38) Masserini, M.; Freire, E.; Palestini, P.; Calappi, E.; Tettamanti, G. *Biochemistry* **1992**, *31*, 2422–2426.
- (39) Mertz, J. A.; McCann, J. A.; Picking, W. D. *Biochem. Biophys. Res. Co.* **1996**, *226*, 140–144.
- (40) Seo, J. H.; Adachi, K.; Lee, B. K.; Kang, D. G.; Kim, Y. K.; Kim, K. R.; Lee, H. Y.; Kawai, T.; Cha, H. J. *Bioconjugate Chem.* **2007**, *18*, 2197–2201.
- (41) De Haan, L.; Hirst, T. R. *Mol. Membr. Biol.* **2004**, *21*, 77–92.
- (42) Tsuji, T.; Watanabe, K.; Miyama, A. *Microbiol. Immunol.* **1995**, *39*, 817–819.
- (43) Lanne, B.; Schierbeck, B.; Karlsson, K. A. *J. Biochem.* **1994**, *116*, 1269–1274.
- (44) Merritt, E. A.; Sarfaty, S.; Vandenaeker, F.; Lhoir, C.; Martial, J. A.; Hol, W. G. *J. Protein Sci.* **1994**, *3*, 166–175.
- (45) Zhang, R. G.; Westbrook, M. L.; Westbrook, E. M.; Scott, D. L.; Otwinowski, Z.; Maulik, P. R.; Reed, R. A.; Shipley, G. G. *J. Mol. Biol.* **1995**, *251*, 550–562.
- (46) Shimazaki, H.; Shinomoto, S. *Neural Comput.* **2007**, *19*, 1503–1527.
- (47) Scott, D. W. *Biometrika* **1979**, *66*, 605–610.
- (48) Fritz, J.; Katopodis, A. G.; Kolbinger, F.; Anselmetti, D. *Proc. Natl. Acad. Sci. U.S.A.* **1998**, *95*, 12283–12288.
- (49) Yuan, C. B.; Chen, A.; Kolb, P.; Moy, V. T. *Biochemistry* **2000**, *39*, 10219–10223.
- (50) Zhang, X. H.; Wojcikiewicz, E.; Moy, V. T. *Biophys. J.* **2002**, *83*, 2270–2279.
- (51) Wong, S. S.; Joselevich, E.; Woolley, A. T.; Cheung, C. L.; Lieber, C. M. *Nature* **1998**, *394*, 52–55.
- (52) Cai, X. E.; Yang, J. *Biochemistry* **2003**, *42*, 4028–4034.
- (53) Lee, C. K.; Wang, Y. M.; Huang, L. S.; Lin, S. M. *Micron* **2007**, *38*, 446–461.
- (54) Gour, N.; Verma, S. *Tetrahedron* **2008**, *64*, 7331–7337.
- (55) Zhang, X. J.; Yadavalli, V. K. *Anal. Chim. Acta* **2009**, *649*, 1–7.
- (56) Seo, J. H.; Kim, C. S.; Hwang, B. H.; Cha, H. J. *Nanotechnology* **2010**, *21*, 8.